AXON VOLTAGE-CLAMP SIMULATIONS

I. Methods and Tests

JOHN W. MOORE, FIDEL RAMÓN, and RONALD W. JOYNER

*From the Department of Physiology and Pharmacology,
Duke University Medical Center, Durham, North Carolina 27710*

ABSTRACT   This is the first in a series of four papers in which we present the numerical simulation of the application of the voltage clamp technique to excitable cells. In this paper we describe the application of the Crank-Nicolson (1947) method for the solution of the parabolic partial differential equations that describe a cylindrical cell in which the ionic conductances are functions of voltage and time (Hodgkin and Huxley, 1952). This method is compared with other methods in terms of accuracy and speed of solution for a propagated action potential. In addition, differential equations representing a simple voltage-clamp electronic circuit are presented. Using the voltage-clamp circuit equations, we simulate the voltage clamp of a single isopotential membrane patch and show how the parameters of the circuit affect the transient response of the patch to a step change in the control potential. The simulation methods presented in this series of papers allow the evaluation of voltage clamp control of an excitable cell or a syncytium of excitable cells. To the extent that membrane parameters and geometrical factors can be determined, the methods presented here provide solutions for the voltage profile as a function of time.

INTRODUCTION

The voltage clamp technique, originally developed for squid axons (Cole, 1949; Hodgkin et al., 1952), has been applied to a variety of other excitable cells. The interpretation of the recorded currents as being proportional to membrane conductance changes depends on the assumption of isopotentiality of that region of membrane from which the current is recorded. Because this requirement of isopotentiality is never fully met (e.g. the resistance of the surface of the axial wire is not low enough or the length of the node must be finite), it is important to evaluate the quality of any voltage clamp technique.

One particular impetus to initiating these studies was concern for the quality of the voltage clamp of a bundle of smooth muscle. A preliminary report of our initial results reflects this interest (Anderson et al., 1971).

The primary purpose of this group of four papers is to develop methods and show some evaluations of the voltage control of cylindrical cells. The first discusses and compares methods of numerical solutions for the equations describing the axon and voltage clamp. The second paper examines the quality of the double sucrose-gap
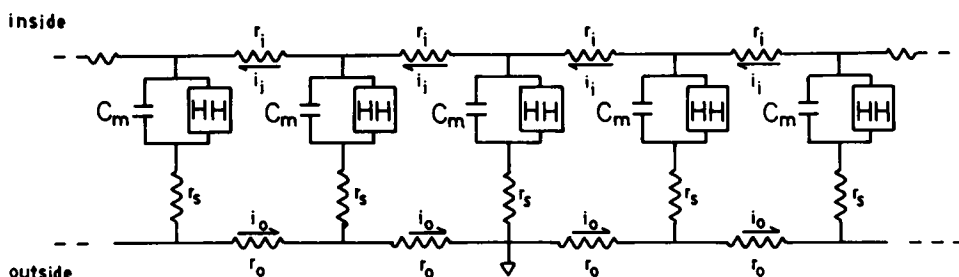
FIGURE 1 Representation of a cylindrical cell as an electrical circuit including the extracellular resistance, (r_o), the axoplasmic resistances, (r_i), the membrane capacitance, (c_m), and the series resistance, (r_s). The active membrane conductances and ionic equilibrium potentials are represented by the boxes marked HH, the Hodgkin and Huxley model.

voltage-clamp which we use.[1] The third paper evaluates the feasibility of voltage clamping in a postsynaptic region of membrane imbedded in an axon, and the fourth treats the problem of a bundle of small axons. These examples are important in the work of our laboratory but the methods are very general and can be easily adapted to simulation and examination of many other experimental arrangements.

A brief description of the components of the system follows.

Cable Equations

Cable equations were derived by Lord Kelvin (1855) to describe voltage and current distribution in the electrical equivalent circuit of the submarine cable. The first to apply them to axons was Weber (1873). Hermann (1877) reduced the problem from three dimensions to one by assuming that radial currents in the core and surrounding medium could be ignored. Several investigators have contributed to the analysis of the corresponding cable equations (Hodgkin and Rushton, 1946, and Lorente de Nó, 1947; for other references see reviews by Taylor, [1963] or Cole [1968]). Fig. 1 represents the electrical properties of long cylindrical nerve cells, such as the squid giant axon as a distributed cable equivalent circuit. The resistance in series with the squid axon membrane first described by Hodgkin et al. (1952) is important in quantitative studies of voltage clamp currents and is included for completeness. However it will be assigned a value of zero until the effect of the series resistance is specifically considered in the fourth paper.

There are numerous derivations of the cable equations; we refer the reader to Cole (1968) (whose sign convention we follow). The membrane voltage (V_m) is taken as inside minus outside voltage and inward current is taken as positive. The subscripts i and o represent the inside and outside, respectively. In the absence of external sources or sinks, the general cable equation is given by

$$\partial^2 V_m / \partial x^2 = (r_i + r_o)(c_m [\partial V_m / \partial t] + [V_m / r_m]), \tag{1}$$

---

[1] A preliminary report has been given at an American Physiological Society meeting (Anderson et al., 1971).

where r_i and r_o are the internal and external resistivities per unit length and i_m and c_m are the membrane current and capacitance per unit length; r_m is the membrane resistance × unit length.

It is frequently expressed in the form

$$\lambda^2(\partial^2 V_m/\partial x^2) = \tau_m(\partial V_m/\partial t) + V_m, \tag{2}$$

where $\lambda^2 = r_m/(r_i + r_o)$ and $\tau_m = r_m c_m$.

Hodgkin and Rushton (1946) assumed the membrane resistance and the injected current to be constant and derived an analytic solution for Eq. 2. This "passive cable" solution will hold for small perturbations about the resting potential, but to obtain a more realistic solution, the nonlinear membrane characteristics of an axon must be incorporated into Eq. 2.

Nonlinear Membrane of the Squid Giant Axon

The Hodgkin and Huxley (H-H, 1952) model is the reference standard description of squid axon membrane ionic conductances. A set of ordinary differential equations describe three independent first order reversible processes whose forward and backward rate constants are voltage dependent. The H-H membrane model may be incorporated into the cable equations, by replacing V_m/r_m in Eq. 1 by the H-H ionic current per unit length of membrane, i_{ion}, giving

$$(1/[r_i + r_o]) \, (\partial^2 V_m/\partial x^2) = c_m(\partial V_m/\partial t) + i_{ion}. \tag{3}$$

The solution of this nonlinear partial differential equation (PDE) cannot be obtained by analytical procedures but Hodgkin and Huxley (1952) transformed it into an ordinary differential equation by assuming that the action potential propagates at a constant speed θ along an axon with constant diameter and membrane properties. This method is not applicable at ends or to regions of changing geometry or membrane properties (e.g. as a result of temperature variations or drug treatment). Therefore it is necessary to solve Eq. 3 by numerical methods. Programs for its solution are now available and can be run on even small laboratory computers.

Voltage Clamp Methods and Characteristics

The Hodgkin-Huxley model was formulated from data obtained from a voltage clamp of the squid giant axon, where longitudinal gradients were avoided by introduction of an axial wire with low surface resistance. The axial wire also provides a low resistance path to supply the required membrane current, the current per unit length being:

$$i_m = c_m(\partial V_m/\partial t) + i_{ion}. \tag{4}$$

If the membrane potential is forced to follow to a voltage step, capacitative current flows only during the period during which the membrane potential is changing. Follow-

ing that, the feedback circuit injects or withdraws the ionic current through the membrane arising from changes in the voltage-dependent ionic conductances.

For a good voltage clamp, the membrane must have a uniform potential over the region from which current is measured. In large axons, this is frequently achieved by means of the previously mentioned short-circuiting axial wire. For voltage clamping small fibers the most widely used technique is the double sucrose gap introduced by Stämpfli (1954) and first used on lobster axons by Julian et al. (1962 *a,b*). The sucrose-gap voltage clamp is based on electrical isolation of a "node" or short length of axon between two high resistance partitions of flowing sucrose. When the node length is short[2] (compared with the diameter), space clamp conditions are approximated—that is, any voltage gradients over the length of the node hopefully introduce only small errors. Since then the method has been applied to several other cells such as squid axons (Moore et al., 1964), smooth muscle (Anderson, 1969), cardiac muscle (Rougier et al., 1968), and skeletal muscle (Moore, 1972; Ildefonse and Rougier, 1972).

Previously a simplified first approach to simulation of a realistic voltage clamp had been carried out by assuming that the cable properties of the axon could be represented by two coupled patches of isopotential membrane (Taylor et al., 1960). Not only was the cable very oversimplified for this simulation but it also left out the control amplifier characteristics as well as the membrane capacitance. The current through one patch was solved by an analog computer and the values "stored" as a line drawn on an X-Y plotter. A curve follower made the stored values available for insertion into the potential signal driving the second patch.

Advances in computer technology since then have made possible the present much more realistic simulations on a digital minicomputer. They incorporate a representation of the full control circuit as well as an accurate description of the axon as a cable, including the membrane capacitance.

LIST OF SYMBOLS

t	Time (s).
k	Time increment, Δt (s).
x	Distance (cm).
h	Spatial increment, Δx (cm).
a	Axon or cable radius (cm).
D	Axon or cable diameter (cm).
R_i	Resistivity of internal medium (Ω-cm).
C_m	Membrane capacitance per unit area (F/cm^2).
V_m	Transmembrane voltage (V).
V_i, V_o	Internal and external voltages with respect to ground (V).

---

[2] When the segment length is comparable to the diameter of the axon, one must consider the three-dimensional voltage distribution problems. Eisenberg and Johnson (1970) showed serious nonuniformities exist for a point source of current injection. In the experiments considered for simulation in this paper, the current entering the segment is distributed across the whole cross section of the axon and we may consider a one-dimensional system with assurance.

i_i, i_o	Internal and external longitudinal currents (A).
r_i, r_o	Internal and external medium resistance per unit length (Ω/cm).
i_m	Transmembrane current per unit length (A/cm).
c_m	Membrane capacitance per unit length (F/cm).
r_m	Membrane resistance × unit length (Ω cm).
λ	Length constant (cm).
τ_m	Time constant (s).
θ	Conduction velocity (cm/s).
i_{ion}	H-H ionic current per unit length (A/cm).

METHODS

Numerical Integration

There are only a few special cases in which the solution to Eq. 2 may be written in closed form, such as an infinitely long passive cable (Hodgkin and Rushton, 1946) or an infinitely long passive cable terminated at one end by a cell body (Rall, 1960). For a passive cable of finite length, the solution for the condition of current injection at a single point can be written as a Laplace transform (Norman, 1972). Solutions for the propagation of transient potentials in a wide variety of finite and infinite passive cables have been obtained (Jack and Redman, 1971) but these solutions are written in closed form only for a current impulse. To obtain the solution for a transient potential resulting from an arbitrary current function, the solution for the current impulse must be convolved with a current function.

Hodgkin and Huxley (1952) transformed the partial differential equation into an ordinary differential equation by assuming that the action potential propagates with constant velocity, obtaining

$$(1/2 [r_i + r_o] \theta^2) \, \mathrm{d}^2 V_m / \mathrm{d}t^2 = c_m (\mathrm{d}V_m / \mathrm{d}t) + i_{ion}.$$

It is possible to solve this equation when θ is known, but it is necessary to find θ by trial and error through iteration. The solution is very sensitive to the value of θ and the solutions diverge to $\pm \infty$ after the peak of the impulse even for θ bracketed to one part in 10^7 (FitzHugh and Antosiewicz, 1959). Hodgkin and Huxley (1952) switched the method of calculation for the falling phase to that for a membrane action potential. FitzHugh and Antosiewicz (1959) were able to extend the solutions to the latter part of the impulse by interpolating between these two bracketing solutions to find initial conditions for continuation of the computation. This procedure "had to be repeated as many as six times" before satisfactory solutions were obtained.

The scheme of transformation of a partial to an ordinary differential equation is restricted to propagation of an impulse with constant velocity along a cylinder of constant diameter.

The more generally useful approach is to write the partial differential equation as a difference equation and solve this. This difference equation may be solved numerically by either explicit or implicit methods of integration. Explicit methods evaluate expressions for partial derivatives of V while implicit methods solve simultaneous equations (relating the potential at several points along the cable) which imply, or are the result of stepwise integration.

The explicit method scheme uses the second central difference at time t for the second partial derivative of V (footnote 3) with respect to x, and the forward difference as the time

---

[3] For simplicity we now consider the axon in a bath large enough for us to neglect the external resistivity. Then the membrane potential is identical with the internal potential and we drop these subscripts.

derivative of V. When this is done, the cable equation (Eq. 3) can be written as:

$$(V_{x-h}^t - 2V_x^t + V_{x+h}^t)/(h)^2 = r_i c_m([V_x^{t+k} - V_x^t]/k) + r_i i_{ion}, \qquad (5)$$

where h is the spatial increment (Δx) and k the time step (Δt). The value of V^{t+k} can be evaluated for each segment because the voltages at all values of x at time t are known, either from previous calculations or as a boundary condition for the first time step. In principle, the solution of any cable equation problem may be obtained by explicit numerical integration, using any one of several methods for derivative evaluations. However, two basic constraints with explicit methods make them unstable and impractical for some axon problems.

The first constraint is that, for stability of numerical solutions of parabolic partial differential equations (including those for cables), the ratio of the increments in time and distance must satisfy the following condition. See for example, Gerald, 1970:

$$D k/4h^2 R_i C_m \leq 0.5,$$

where D is the axon diameter in centimeters.

When the axon membrane is characterized by temporal and voltage dependent conductances (e.g. the H-H membrane), a second stability condition must also be met. The integration time step must be short compared to the time constant of the changes in the membrane conductance, i.e. the k/τ_m ratio should also be less than 0.3. For an accurate solution, one would imagine that this ratio would have to be much smaller.

To illustrate this problem let us consider explicit numerical integration using axon segment lengths equal to the diameter ($500\mu m$), the first condition requires that the time step must be $\leq 3\ \mu s$. This makes the solution quite slow because some 3,000 computation loops are required at each segment for a reasonable length of membrane time (10 ms at 6.3°C). While this may be acceptable for studies of impulse propagation over a length of axon, accurate simulations of the voltage profile in a short length of axon (such as 1/4 to 1/2 the axon diameter for a sucrose gap) require much shorter segments. Whenever the segment length is halved, the time interval must be reduced fourfold to maintain stability. This rapidly leads to a situation requiring extremely short time steps and correspondingly unacceptable computation times.

When the simulation includes the additional complication of the voltage control circuit in explicit numerical integration, still another difficulty arises. The potential at the point of current injection tends to swing wildly and lead to unstable solutions because computations for the potential of this input segment are made without relation to its neighbors.

On the other hand, implicit methods of integration are intrinsically stable and ideally suited for solution of parabolic partial differential equations such as those for the cable (Young, 1961). In contrast to the explicit method, there is no restriction on the relative sizes of the temporal and spatial steps. In these methods the voltage distribution over the whole length of the cable is calculated for each time step. For stability of simulations which include the voltage control, implicit methods of numerical integration are almost the required method.

The first numerical solutions of the equations for impulse propagation in an axon with a Hodgkin-Huxley membrane were made by Cooley and Dodge (1966) with an implicit integration method based on the trapezoidal rule. The method used in the present work is the Crank-Nicolson (1947) implicit method and is similar to that used by Heppner and Plonsey (1970).[4]

Briefly, the Crank-Nicolson method of integration consists of writing the differential equation as a difference equation for each segment, with the second order spatial derivative replaced with the second central difference at the present time step (t) and at one time increment later

$(t + k)$. If the voltage at time t in cable segment j is written as V_j^t, then the difference equation for segment j is:

$$r_i c_m [V_j^{t+k} - V_j^t)/k] = [1/2(h)^2][V_{j-h}^t - 2V_j^t + V_{j+h}^t$$
$$+ V_{j-h}^{t+k} - 2V_j^{t+k} + V_{j+h}^{t+k}] - r_i i_{ion}, \quad (6)$$

where, as before, h represents the increment in distance and k the increment in time. Boundary conditions must be stated for the first (F) and last segment (L) to represent the terminations of the cable. We take the condition of perfect end sealing or zero longitudinal current flow to the left end and zero current to the right end, i.e.

$$V_F = V_{F-1} \quad \text{and} \quad V_L = V_{L+1}.$$

These assumed boundary conditions approximate the situation for several voltage clamp arrangements of interest: (1) The central guarded segment of an axon with an axial wire having a low surface resistance. (2) The ends of the artificial node in a sucrose gap with negligible external leakage. (3) An axon with an internally injected oil drop electrically sealing off an end. (4) The termination at the end of a long cable because boundary conditions here do not affect potentials at several "length constants" away.

For all segments except the terminal ones:

$$-KV_{j-1}^{t+k} + 2(1 + K) V_j^{t+k} - KV_{j+1}^{t+K} =$$
$$2(1 - K) V_j^t + K(V_{j-1}^t + V_{j+1}^t) - (2K/c_m)i_{ion}, \quad (7)$$

where $K = k/r_i c_m h^2$. The terminal segments are evaluated separately. The first segment is given by:

$$-KV_{F+1}^{t+k} + 2(1 + K/2)V_F^{t+k} = KV_{F+1}^t + 2(1 - K/2)V_F^t - (2k/c_m)i_{ion}, \quad (8)$$

and for the last segment, segment L

$$-KV_{L-1}^{t+k} + 2(1 + K/2) V_L^{t+k} = KV_{L-1}^t + 2(1 - K/2) V_L^t - (2k/c_m)i_{ion}. \quad (9)$$

Note that the equations are arranged such that the left side includes only terms containing the voltage at the next time step, and that the right side includes only terms containing the voltage and the current at the present time step, which are assumed to be known. When the first segment is taken as segment 1, these equations can now be written in matrix form as:

$$\begin{bmatrix} c_1 & b_1 & 0 & 0 & & & \\ a_2 & c_2 & b_2 & 0 & 0 & & \\ 0 & \cdot & \cdot & \cdot & 0 & 0 & \\ 0 & 0 & \cdot & \cdot & \cdot & 0 & 0 \\ & 0 & 0 & \cdot & \cdot & \cdot & 0 \\ & & & a_{L-1} & c_{L-1} & b_{L-1} \\ & & & & a_L & c_L \end{bmatrix} \times \begin{bmatrix} V_1^{t+k} \\ V_2^{t+1} \\ \cdot \\ \cdot \\ \cdot \\ V_{L-1}^{t+k} \\ V_L^{t+k} \end{bmatrix} = \begin{bmatrix} d_1 \\ d_2 \\ \cdot \\ \cdot \\ \cdot \\ d_{L-1} \\ d_L \end{bmatrix}$$

where the a's, b's, and c's are constants related to the cable parameters and the d's are functions of the membrane potential and current at the current time step (i.e., the right sides of Eqs. 7, 8, and 9). Since we have L equations in L unknowns (the voltages at the next time step), if the d's are computed at each time step we can solve for the unknowns by standard matrix methods of inversion or elimination. Because the matrix is tridiagonal, a particular modification of the Gauss-Seidel elimination method can be used (Gerald, 1970).

Evaluation of Accuracy of Solutions of the PDE

It is possible to obtain an analytical solution for passive cables. We tested our integrations for an ohmic membrane against error function solutions for an infinite cable (Hodgkin and Rushton, 1946) and found them to superimpose.

However there are no analytical solutions for the nonlinear partial differential equation such as a cable with an excitable membrane and therefore it is not possible to make comparisons of computations by any particular method with the "true" solutions. However there are a few practical ways to assess the validity of the computed solutions: (1) They must not violate physical principles. (2) They must satisfy the original PDE. (3) They may be compared[5] to solutions by different time and distance increments. (4) They may be compared[5] to solutions by different integration methods.

The first two tests were readily satisfied. The most sensitive variable to compare integration methods and increment sizes appears to be the speed of impulse propagation. Table I compares different methods of integration for a propagating action potential in an axon with an

TABLE I

METHODS OF INTEGRATION FOR A PROPAGATING ACTION POTENTIAL IN AN AXON WITH AN H-H MEMBRANE

	Uniform wave assumption	Explicit		Implicit	
		Euler,* 1st order	Euler,* 2nd order	Trapezoidal ‖	Crank-Nicolson*
dt (μs)		5	1	1	10	10
Speed (m/s)	18.8‡ 18.74§ 18.74339 ‖ 18.7274*	49.5	21.24	21.19	18.694	18.795
V_p (mV)	90.55*	102.34	92.70	92.62	90.5	90.68
dV/dt (V/s)	429.9*	547.52	475.61	473.16		438.43
Relative computation time		10	10			1

Where applicable, segment lengths of 500 μm were used for all methods and the number of segments was 100 (ours) or more.
*Present work.
‡Hodgkin and Huxley, 1952.
§FitzHugh and Antosiewicz, 1959.
‖ Cooley and Dodge, 1966.

---

[5] A similar evaluation for solutions of the ordinary differential equations describing the Hodgkin-Huxley model for a uniform patch of membrane has been made for membrane action potentials by numerical integration. Moore and Ramón (*J. Theor. Biol.*, 1974) found that as the time increment decreased, the solutions approached an invariant solution which was identical for all integration methods tested.

H-H membrane. The parameters used for the comparison were: the speed of propagation of the action potential once it attains its constant value, the spike height (V_p) and the maximum rate of rise (dV/dt). The cable and integration parameters, where applicable, were the same: radius of 238 μm, axoplasm resistivity 35.4 Ω-cm, temperature 18.5°C and dx of 500 μm.

The simplified ordinary differential equation method of Hodgkin and Huxley (1952) presumably would yield an accurate value of the constant speed of propagation for the action potential if the integration of the ordinary differential equation is accurate (see for example, Moore and Ramón, 1974). The speed of propagation obtained from the uniform wave assumption falls between those found by two implicit methods of integration and differs from them by only about 5 parts in 2,000. Cooley and Dodge (1966) have shown (their Table I) that as the spatial increment is decreased the velocity found by their implicit method moves even closer to the wave equation solution but a decrease in the time step makes little change in the velocity. Because our implicit solution falls so close to theirs, we have not repeated their systematic evaluation. In contrast, explicit methods, using the same time step fail badly and it is only when the time steps are reduced 10-fold that they yield values that approach those from other methods. The time to compute one increment in axon time is about the same for each of the methods examined. Therefore the explicit methods which require a small step size take much more computer time to approach the proper velocity of propagation, revealing another distinct disadvantage of the explicit methods. Although the ODE resulting from the wave equation assumption can be solved rapidly, a very large number of iterations is required in order to obtain a solution through most of the falling phase of the action potential. Thus the overall computation time may often exceed even that for integration of the PDE.

Voltage Clamp Equations

The voltage clamp circuit frequently used in our laboratories (Moore et al., 1964; Moore, 1965) is represented in Fig. 2. There are several lag response elements in the feedback circuit: (*1*)
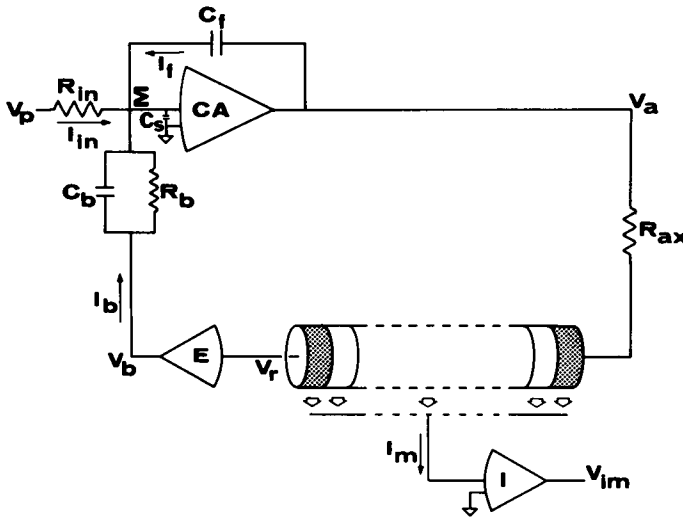

FIGURE 2 Diagram of the voltage clamp circuit to be simulated; showing the control amplifier, (*CA*), and the feedback loop which includes the cell and the current measuring amplifier, (*I*). The current from *CA* enters the cell through a resistance, (R_{ax}), and the potential of one segment is measured by the amplifier, (*E*), and fed back to the summing point of *CA*.

the transient response of the control amplifier; (2) the lag of the voltage across the membrane capacitance behind the injected current; (3) the lag in the spread of potential along the cable from the segment of current injection to the segment where potential is recorded; (4) the lag of the potentiometric or electrometer amplifier in measuring the membrane potential. Where the potential is measured through a resistance of less than 1 MΩ (as in a sucrose gap), this lag usually has a time constant of less than 5 μs and we have neglected it in simulations. In circuits where measurements are made via high resistance micropipette electrodes, one should consider including it in the simulation as a first or second order response. Where two micropipettes are used, one for current injection and one for potential measurement, the capacitance between them may be the most important element in the circuit and needs to be included in the simulation.

The net effect of these lags is to introduce a total phase lag in excess of 180° at high frequencies. Therefore the system will oscillate unless phase lead is introduced or the system gain is reduced to below unity before the high-frequency phase lag reaches 180°. In order to have an experimental system which is fast but stable, we have regularly introduced C_b to provide phase lead and C_f to attenuate the high frequency gain.

The currents which flow to and from the control amplifier in Fig. 2 are defined as follows:

$$I_{in} = V_p - \epsilon/R_{in}, \tag{10}$$

$$I_f = C_f(d[V_a - \epsilon]/dt), \tag{11}$$

$$I_b = (V_b - \epsilon/R_b) + C_b(d[V_b - \epsilon]/dt), \tag{12}$$

$$I_s = C_s(d\epsilon/dt). \tag{13}$$

Applying conservation of charge to the summing point of the control amplifier, we have the differential equation for ϵ, the potential at the summing point

$$(C_b + C_f + C_s)(d\epsilon/dt) = (V_p - \epsilon/R_{in}) + (V_b - \epsilon/R_b)$$
$$+ C_b(dV_b/dt) + C_f(dV_a/dt). \tag{14}$$

The differential equation describing the control amplifier itself is

$$dV_a/dt = -(\epsilon \cdot A_o + V_a)/\Upsilon_a, \tag{15}$$

where the amplifier's low-frequency open loop gain is $-A_o$ and its time constant is Υ_a. The following steps are carried out for each time increment: (1) Eqs. 14 and 15 are integrated to give V_a (the maximum output is limited to ±10 V). (2) the current applied through the access resistance (R_{ax}) is calculated from the voltage difference between the output of the control amplifier and the voltage of the membrane at the segment of the current injection. (3) The potential distribution throughout the cable is determined by the implicit integration method. (4) The new voltage in the segment of the cable where potential measurement is simulated, labeled V_b, is available for use in Eq. 14 for the next iteration.

SIMULATION RESULTS AND TESTS

We will develop our observations in such a way as to try to separate and clarify the contributions of the various components to the observations made in the most complex situation. We start with an oversimplified system and increase the complexity in a

Parameter	Squid (500 μm)	Lobster (125 μm)
A_o	500,000	500,000
τ_a	10 μs to 1 ms	10 μs to 1 ms
R_{in}	10 KΩ	10 KΩ
R_{ax}	20 KΩ	50–750 KΩ
R_b	50 KΩ	50 KΩ
C_b	0.5×10^{-9} F	0.1×10^{-9} F
C_f	0.085×10^{-9} F	0.05×10^{-9} F

stepwise fashion, using more realistic assumptions at each step. For the purposes of studying the stability (control of oscillations) of the voltage clamp, we will first consider lumped passive isopotential patches of membrane, then we will include membrane excitability in an isopotential segment. The following papers consider distributed excitable membrane in several voltage-clamp arrangements.

Voltage Clamp of Passive Patch

The first test of the voltage-clamp circuit simulation was made with parameters chosen to fit specific experimental situations of special interest in our laboratory. We frequently use squid and lobster axons in a double sucrose-gap chamber, the length of the exposed axon in the "artificial node" is usually less than or equal one-half the axon diameter. Typical parameter values which we have used, needed, or observed for the circuit are given in Table II.

The values of C_f and C_b may be adjusted to obtain the fastest voltage-clamp for each particular cable model as is frequently done for each experiment. Fig. 3 illustrates how the transient voltage response to a step command changes from underdamped to overdamped as the value of C_b is increased. Typical values for a passive patch of a
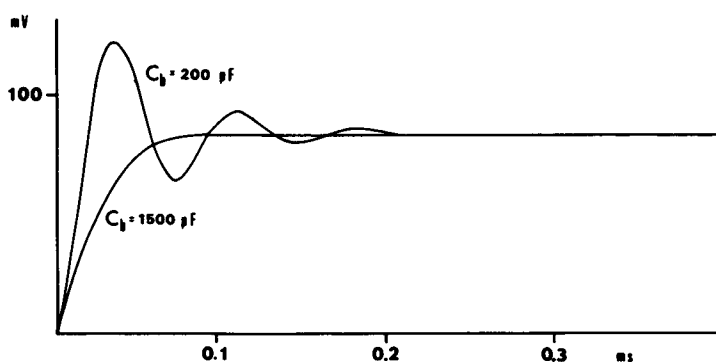

FIGURE 3 Transient voltage clamp response (to a 75 mV step command) of a passive membrane patch of diameter 500 μm, length 250 μm, and specific membrane resistance 1000 Ω-cm^2, using two values for the capacitance C_b in the voltage clamp circuit of Fig. 2.

500 μm diameter squid axon 250 μm in length with a specific membrane resistance 1,000 Ω-cm^2 were used.

Clamped Excitable Membrane

We next endow a membrane patch with the reference standard characteristics for the squid axon described by the Hodgkin and Huxley (1952) equations and assume that it is isopotential throughout. In so doing we simulate the original voltage clamp experiments of squid axons (Cole, 1949; Hodgkin et al., 1952) in which a nearly uniform potential was maintained over a considerable length by means of a short-circuiting axial wire with a low surface resistance. Because voltage clamp experiments in our laboratory frequently yield ionic current densities which are twice as large as those given by the H-H equations (Hodgkin and Huxley, 1952), we scaled up the maximum conductance two-fold, taking $\bar{g}_{Na}$ = 240 mmho/cm^2 and $\bar{g}_K$ = 72 mmho/cm^2 à la FitzHugh and Cole (1964).

For the active patch, the membrane conductances change as function of voltage and time. Following a step command to the control circuit, the potential measured by the electrometer amplifier becomes voltage-clamped after some delay due to the time to charge the capacitance through the access resistance. The patch then undergoes the well known changes in conductance associated with the depolarizing potential step. In order to keep the voltage across the membrane at the command potential, the control amplifier has to inject or withdraw current equal to that flowing through the membrane. To generate the current flow, the output voltage of the control amplifier deviates from the desired value, first in the negative direction during the phase of inward
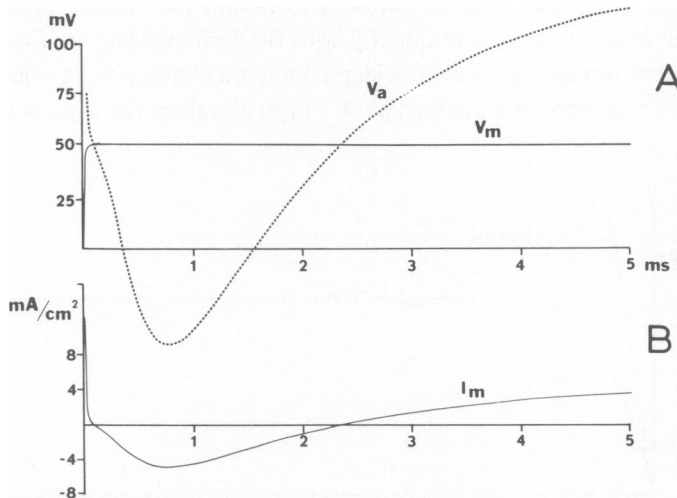

FIGURE 4 Current and voltage response from an active membrane patch of diameter 500 μm and length 250 μm. The upper part (A) shows the transmembrane voltage (V_m) along with the output voltage of the control amplifier (V_a). The lower part (B) is the current elicited from the membrane in response to the 50 mV depolarizing step.

current and later in the positive direction during the outward current. The waveform of the control amplifier output deviations appears to be rather similar to that of the ionic current through the clamped membrane, but the amplitude depends on the access resistance R_{ax}.

The results of such a simulation (using the same size patch and control circuit parameters as in Table II) are shown in Fig. 4. The membrane voltage undergoes a step depolarization of 50 mV from rest and remains constant throughout the 5 ms shown in the figure. After the initial transient, the output voltage of the control amplifier (V_a shown in Fig. 4 A) follows a pattern which is the sum of the potential step and the current generated by the membrane segment (Fig. 4 B). The peak inward and steady-state outward current-voltage relations obtained when the command is stepped from a 20 mV hyperpolarized holding potential to several potentials over the physiological range are essentially identical to those which obtain from the augmented H-H equations under assumed perfect voltage-clamp conditions.

REFERENCES

ANDERSON, N. 1969. *J. Gen. Physiol.* **54**:145.
ANDERSON, N., F. RAMÓN, and J. W. MOORE. 1971. *Physiologist.* **14**:102.
COLE, K. S. 1949. *Arch. Sci. Physiol.* **3**:253.
COLE, K. S. 1968. Membranes, Ions and Impulses. University of California Press, Berkeley.
COOLEY, J. W., and F. A. DODGE. 1966. *Biophys. J.* **6**:583.
CRANK, J., and P. NICOLSON. 1947. *Proc. Cambridge Phil. Soc.* **43**:50.
EISENBERG, R. S., and E. A. JOHNSON. 1970. *Prog. Biophys. Mol. Biol.* **20**:1.
FITZHUGH, R., and H. A. ANTOSIEWICZ. 1959. *J. Soc. Ind. Appl. Math.* **7**:447.
FITZHUGH, R., and K. S. COLE. 1964. *Biophys. J.* **4**:257.
GERALD, C. F. 1970. Applied Numerical Analysis. Addison-Wesley Publishing Co., Inc., Reading, Mass.
HEPPNER, D. B., and R. PLONSEY. 1970. *Biophys. J.* **10**:1057.
HERMANN, L. 1877. *Pfluegers Arch. Gesamte Physiol.* **15**:191.
HODGKIN, A. L., and A. F. HUXLEY. 1952. *J. Physiol. (Lond.).* **117**:500.
HODGKIN, A. L., A. F. HUXLEY, and B. KATZ. 1952. *J. Physiol. (Lond.).* **116**:424.
HODGKIN, A. L., and W. A. H. RUSHTON. 1946. *Proc. R. Soc. Lond. B.* **133**:444.
ILDEFONSE, M., and O. ROUGIER. 1972. *J. Physiol. (Lond.).* **222**:373.
JACK, J. J. B., and S. J. REDMAN. 1971. *J. Physiol. (Lond.).* **215**:283.
JULIAN, F. J., J. W. MOORE, and D. E. GOLDMAN. 1962 *a. J. Gen. Physiol.* **45**:1195.
JULIAN, F. J., J. W. MOORE, and D. E. GOLDMAN. 1962 *b. J. Gen. Physiol.* **45**:1217.
KELVIN, LORD (WILLIAM THOMPSON). 1855. *Proc. R. Soc. Lond.* **7**:382.
LORENTE DE NÓ, R. 1947. Studies from The Rockefeller Institute, New York. Vols. 131, 132.

MOORE, J. W. 1965. *J. Gen. Physiol.* **48**:11.

MOORE, J. W., T. NARAHASHI, and W. ULBRICHT. 1964. *J. Physiol. (Lond.).* **172**:163.

MOORE, J. W., and F. RAMÓN. 1974. *J. Theor. Biol.* **45**:249.

MOORE, L. E. 1972. *J. Gen. Physiol.* **60**:1.

NORMAN, R. S. 1972. *Biophys. J.* **12**:25.

RALL, W. 1960. *Expt. Neurol.* **2**:503.

ROUGIER, O., G. VASSORT, and R. STÄMPFLI. 1968. *Pfluegers Arch. Eur. J. Physiol.* **301**:91.

STÄMPFLI, R. 1954. *Experientia.* **10**:508.

TAYLOR, R. 1963. *In* Physical Techniques in Biological Research. W. L. Nastuk, editor. Academic Press, New York. Vol. 6. Chap. 4.

TAYLOR, R. E., J. W. MOORE, and K. W. COLE. 1960. *Biophys. J.* **1**:161.

WEBER, H. 1873. *J. Reine Angew. Math.* **76**:1.

YOUNG, D. 1968. *In* Modern Mathematics for the Engineer. 2nd series. E. F. Beckenbach, editor. McGraw-Hill Book Company, New York. 373.